

ESTERFIP, A TRANSESTERIFICATION PROCESS TO PRODUCE BIO-DIESEL FROM RENEWABLE ENERGY SOURCES

A. Hennico, J. A. Chodorge and A. Forestière

INSTITUT FRANCAIS DU PETROLE
RUEIL-MALMAISON (92500), FRANCE

Keywords : Transesterification, Vegetable Oils, Bio-Diesel.

1 - INTRODUCTION

Vegetables oils and products synthesized from natural raw materials (either of vegetable or animal origin) are having a strong "come back" in the recent decades. One of the major reasons for the increased utilization of fatty chemicals for industrial use has been the ability to tailor the products to specific needs. This trends is clearly indicated in Table 1 that gives an estimate of the world fat production in millions tons and in the case of vegetable oils, the yields per unit area (hectare) per year.

End uses of upgraded products or derivative compounds are extremely numerous but usually highly specialized. Major areas of applications are :

Food industry, soap and detergents, cosmetics, pharmaceuticals, textile and paper industry, oil field chemicals, fat based emulsifiers, synthetic lubricants, metal working fluids and last but not least introduction into the automotive fuel sector. This last application will be the subject of this presentation.

In the early days of diesel engines, vegetable oils were tested (their original compositions unchanged) as a possible motor fuel but the idea never took hold owing to incompatibility problems such as deterioration of the oil with time, high viscosity, and fouling of the engine.

Recently the bio-diesel route has been reactivated for a number of reasons as outlined hereafter :

- It has been found that vegetable oil can be transformed via esterification into a product which is much more adequate as a diesel fuel than the original oil itself.
- A wide variety of vegetable oils can be used as raw material for transesterification; this has led to the idea that bio-diesel production could be a way to extend the role of agriculture (more jobs created and reduced financial burden for petroleum imports in developing countries, slow-down in the current reduction of cultivated surfaces for developed countries like those of the European community).

2 - THE ESTERFIP PROCESS DEVELOPED BY IFP* FOR THE TRANSESTERIFICATION OF VEGETABLE OILS

Transesterification of natural glycerides with methanol to methylesters is a technically important reaction that has been used extensively in the soap and detergent manufacturing industry. IFP has done extension R and D work in the transesterification field with the aim of creating a product that would be suitable as an excellent substitute for diesel fuel.

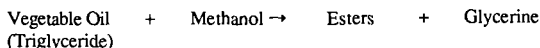
As a result, a new process called ESTERFIP was developed that allows the elimination of certain impurities from the product that otherwise would be detrimental to classical diesel engines.

The ESTERFIP process was developed by IFP first on a laboratory scale, then tested in a pilot plant (1987) and demonstrated in a commercial plant that is operating satisfactorily since 1992 (capacity 20 000 t/yr). Originally the design was developed for batch operation which is very suitable for small capacities and then further upgraded to continuous operation, an economically dictated choice for intermediate and large capacities.

2 - 1 Chemistry Involved

The reaction of transesterification involves the reaction of methanol with the triglycerides of the rapeseed oil to form the corresponding methylesters and glycerine as indicated on the following reaction scheme :

* Jointly with Sofiproteol (France)



This global stoichiometry is of course an oversimplification as we are in presence of a three-step reversible reaction with di- and monoglycerides as intermediate products. The reaction takes place in presence of a catalyst that is most commonly sodium hydroxide, potassium hydroxide or sodium methylate. In the case of bio-diesel manufacturing, the main objective is to achieve the maximum possible conversion towards methylester (in excess of 97 %). This aim puts certain specific constraints on the reaction scheme, such as long hold-up time or eventually unreacted feed components recycling, involving a difficult separation between reactants and product.

Furthermore to avoid operating problems in the ESTERFIP process the vegetable oil used as feedstock should be partially refined to eliminate phospholipides, gummy substances, free acid and water.

Typical feed specifications are :

- Phosphorous content : 10 ppm wt maximum
- Water content : 0,1 wt % maximum
- Acidity index : 1 maximum

The situation is also complicated by solubility problems. For example in the present case neither methanol is soluble in the starting material triglyceride nor the end products glycerine and fatty acid methyl esters are miscible, whereas methanol is soluble in fatty acid methyl esters. We can therefore expect different time dependent situations - at the beginning a two-phase system, followed by an almost complete solution. Then as soon as a considerable amount of glycerine is formed, a new two phase system will again prevail.

2 - 2 Composition of Fatty Acids in three common Vegetable Oils

Whereas in Europe methylesters from rapeseed oil and sunflower oil are the most common feedstocks for bio-diesel the US leans heavily upon soybean oil as raw feedstock.

The Table 2 gives the composition of three of the most common renewable vegetable sources that are used in the preparation of bio-diesel.

Although the feed composition is quite different, a careful selection of operating conditions (t, p) and amount of catalyst used permits the production of a bio-diesel that satisfies the most stringent specifications required by the automobile industry.

It is however important here to stress the importance of experimental data checking and unit modeling based upon practical experience, before undertaking the conceptual design of a large size industrial unit.

2 - 3 ESTERFIP Process Description (continuous scheme)

A complete block flow scheme is given on Figure 1. The sequence of processing steps is as follows:

- Transesterification of the vegetable oil by dry methanol in presence of a basic catalyst.
- Decantation to completely separate methyl esters from glycerine.
- The ester phase is water-washed and purified in a continuous operation in order to eliminate the last traces of catalyst particles. This step is very critical to avoid harmful deposits during the combustion in the diesel engine.
- Vacuum evaporation of the methyl ester product to recover traces of methanol and water.
- The raw glycerine recovered in the settler is evaporated (the main methanol removal step), neutralised, decanted to separate fatty acids, and finally completely freed from methanol.

2 - 4 Overall Material Balance (Rapeseed Oil Case)

Refer to Figure 2.

2 - 5 Product Properties

Bio - Diesel (Methyl esters)		Glycerine (by - product)	
Specific gravity	0.88	Glycerine content, wt %	> 80
Flash point, °C	55	Ash content, wt %	< 10
	mini		
Cetane number	49	Other organic compounds, wt %	< 2.5
CFPP, °C	- 12	Methanol content, wt %	< 0.2
Viscosity (cSt 20°C)	7.52	Water content	< 10

2 - 6 Bio-Diesel based Commercial Fuels in France

In the diesel fuel application two main blends of methyl esters are currently commercialised in France, namely :

- A 5 % mixture of bio-diesel in conventional diesel which is for sale to the public in service stations (without distinctive labelling obligation)
- 30 to 50 % mixtures of bio-diesel for use in bus fleets run by municipalities.

The estimated tonnage of bio-diesel commercialised in France for the total year 1994 is 150,000 Tons.

2 - 7 Environmental Advantages of Bio-Diesel

The main distinctive features of bio-diesel versus conventional diesel fuel are :

- No sulphur
- No aromatics
- Presence of oxygen in the molecular composition
- Renewable energy.

The engine emissions are sulphur free and the other exhaust components are given (on a comparative basis with conventional diesel) in Figure 3.

3 - CONCLUSIONS

Bio-diesel is at present the most attractive market among the non-food applications of vegetable oils. The different stages in the production of rapeseed methyl ester generate by-products which offer further outlets. Oil cake, the protein rich fraction obtained after the oil has been extracted from the seed is used for animal feed.

Glycerol, the other important by-product has numerous applications in the oil and chemical industries such as the cosmetic, pharmaceutical, food and painting industries. New applications are under investigations.

The bio-diesel market in the European Union has a very strong potential growth position due to special fiscal measures that are already applied in several countries and under serious considerations in others.

TABLE 1 - ESTIMATED WORLD VEGETABLE OIL + FAT PRODUCTION

	Production (10 ⁶ T) (1)			Yield, metric t/ha per year
	1980	1990	2000	
Soybean	14.4	16.9	23.2	0.2 - 0.6
Rapeseed (canola, colza)	3.4	8.1	10.7	1.5 - 2
Palm	4.7	10.6	17.4	5 - 8
Sunflower	5.6	8.0	9.9	1 - 1.5
Coconut	3.0	3.0	3.3	3 - 4
Sesame	0.7	1.3	2.1	0.2
Others	11.4	12.7	15.3	
Total	43.2	60.6	81.9	
Animal fat	16.1	18.6	21.5	

TABLE 2 - COMPOSITION OF FATTY ACIDS AND METHYL ESTERS

	* C16:0	C18:0	C18:1	C18:2	C18:3	C20:0	C20:1	C22:0	C22:1
FATTY ACIDS	Palmitic	Stearic	Oleic	Linoleic	Linolenic	Arachidic	Gadoleic	Behenic	Erucic
methyl ester oil	%	%	%	%	%	%	%	%	%
methyl ester	5	2	59	21	9	< 0,5	1	< 0,5	< 1
Rapeseed oil									
methyl ester	10	4	23	53	8	< 0,5	< 0,5	< 0,5	—
Soybean oil									
methyl ester	7	4	22	65	< 0,5	< 0,5	< 0,5	< 0,5	—
Sunflower									

*Cx : y : hydrocarbon chain with X = a number of carbon atoms and Y the number of double bonds.

(1) : A.J. Kaufman + R.J. Ruebusch, J. Amer. Oil Chemist's Soc. - Inform 1, 1034 (1990)

Figure 1
Esterfip Process-Block Diagram

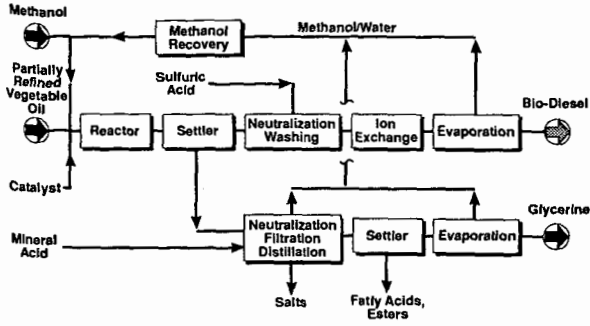


Figure 2
Overall Material Balance (Rapeseed Oil Case)

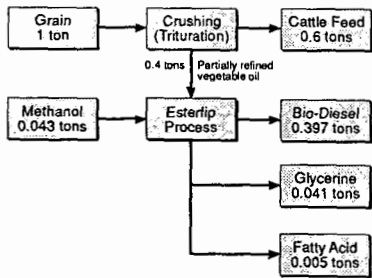
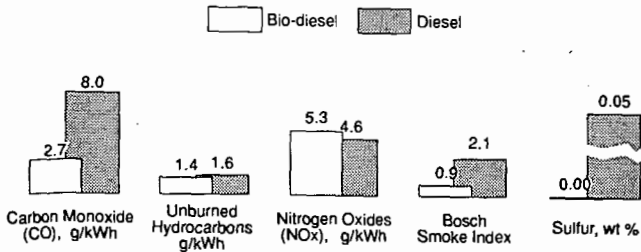


Figure 3
Exhaust Emissions Compared: Bio-Diesel vs Diesel



INVESTIGATIONS ON REDUCING THE BENZO(A)PYRENE CONTENT OF COAL-TAR PITCH

Janusz Zielinski, Blandyna Osowiecka
Technical University of Warsaw
Institute of Chemistry
ul. Lukasiewicza 17
09-400 Plock, Poland

Jerzy Polaczek
Research Institute of Industrial Chemistry
ul. Rydygiera 8
01-793 Warsaw, Poland

George Gorecki
Brent America, Incorporated
921 Sherwood Drive
Lake Bluff, IL 60044

Keywords: benzo(a)pyrene, coal-tar pitch.

Introduction

Bitumens, like coal-derived tars and pitches, as well as petroleum asphalts, have been widely used in many branches of industry and economy [1]. A dramatic limitation of the application areas for bitumens of coal origin is currently observed, due to the carcinogenic action of some bitumen-containing polycyclic aromatic hydrocarbons, especially benzo(a)pyrene (BAP). This hazardous condition was the reason for shutting down plants involved in the coking of coal-tar pitch in Poland and Germany [2,3]. As a result, many research studies on decreasing BAP content in bitumen materials have been performed.

According to literature reviews [4], a considerable reduction in BAP content could be achieved by changing the conditions under which coal-tar pitch is manufactured, especially by decreasing the coal coking temperature [5]. Other workers [6,7] have attained lower BAP concentrations by modifying the pitch properties through oxidation, ultraviolet irradiation [8], or by extraction with low-boiling solvents [8,9]. Polymers not only improve the properties and applicability of bitumen-containing materials [1], but also can play an important role in decreasing their carcinogenicity. The current work studies how the properties of coal-tar pitch are affected by specific high molecular weight substances at elevated temperatures.

Experimental

The following materials were used: Polish coal-tar pitch (R & B softening point, 68.5°C; toluene insolubles, 17.2% w/w; BAP content, 1.83% w/w), suspension-grade polyvinyl chloride (PVC, molecular weight, 139,000; Fikentcher number, 66.9), polystyrene (PS, molecular weight, 304,000; Vicat softening point, 103°C), polyethylene terephthalate waste (PET) and unsaturated polyester resin (UPR, 40-50% styrene solution).

The study was performed stepwise. In the first step, the pitch was heated at 150 to 430°C for 6 h to determine the effect of temperature on the pitch properties. The procedure was executed both with and without removal of distillate. In the second step, the molten pitch was blended with the various polymers: with PVC from between 120 and 350°C for 0.5 to 4 h, with PS from between 240 and 350°C for 0.5 to 4 h, with PET from between 260 and 350°C for 1 to 6 h, and with UPR at 160°C for 3 to 5 h. The products were analyzed for softening and dropping points, penetration (temperature relationship), as well as for BAP content and the amount of toluene-insoluble material. The BAP content was determined using the UV-VIS spectroscopic method [10].

Results and Discussion

The results (Table I) show that the structural changes in the heated pitch are demonstrated by a decrease in penetration and increases in softening point, dropping point and toluene-insolubles content. Changes in these properties became substantial in systems whose temperature was greater than 380°C. The observed decrease in BAP content from 1.83% to 1.48% w/w was not caused by its evaporation because no BAP was found in the distillate fractions. There was very little change in the BAP content for pitch mixtures heated at temperatures below 380°C. As a result, the changes in BAP content in this temperature range can be explained only by chemical interactions between the polymer and the pitch.

It has been found that homogeneous pitch-polymer blends can be obtained under the following conditions:

- an anthracene oil or dibutyl phthalate-plastified PVC up to 10% w/w and below 130°C,
- PS up to 10% w/w and below 310°C,
- PET and UPR, each up to 30% w/w and below 260°C,
- UPR up to 30% w/w and at 110°C, and after subsequent crosslinking at 140 to 160°C.

An individual selection of blending parameters, however, was necessary for each polymer. Temperature was an especially important property. It can be assumed that the elevated temperature contributes to an increase in the amount of toluene-insoluble material. This is due to a simultaneous destruction of polymer molecules and the polycondensation of pitch components, which is also evidenced by an increase of softening point and a decrease of penetration. No correlation, however, between this occurrence and a change in BAP content has been observed.

The largest reductions of BAP content were achieved with pitch-polymer blends containing either PET at 30%; UPR at 30%; or a system comprised of PVC at 4.76%, anthracene oil at 22.63% and butadiene-styrene copolymer latex at 4.76%. The corresponding decreases in BAP content were 72%, 80-90%, and 46%, respectively. Amounts of polyester additive and the effect on BAP content in coal-tar pitch are presented in Fig. 1. The polyester resin used in these compositions was modified additionally by initiators: naphthenate cobalt and hydroperoxide of methyl ethyl ketone. The substantial decrease in BAP content in the case of UPR modification was independent of crosslinking of the resin. The changes in BAP content are likely connected to some chemical interactions between the pitch and the polymer. It has also been found that the plastified PVC-containing pitches can be used in many applications, such as the manufacture of insulating and sealing materials for the building industry [1].

This investigation was sponsored by the Scientific Research Committee and realized as Project No. 7 S203 009 05.

References

1. J. Zielinski, G. Gorecki, "Utilization of Coal-Tar Pitch in Insulating-Seal Materials," ACS Division of Fuel Chemistry, Chicago, 1993, p. 927.
2. J. Jastrzebski, *et. al.*, **Koks, Smola, Gaz**, 1985, **30**, 5.
3. G. Nashan, **Erdol, Erdgas, Kohle**, 1993, **109**, 33.
4. J. Zielinski, *et. al.*, **Koks, Smola, Gaz**, in press.
5. W. Boenigk, J.A. Stadelhofer, "Coal-Tar Pitches with a Reduced Low Molecular PAH Content," 5th International Carbon Conference, Essen, 1992, p. 33.
6. E.A. Sukhorukova, *et. al.*, **Koks, Khim.**, 1984, **7**, 36.

7. W.A. Lebedev, *et. al.*, *Carbon*, 1988, **8**, 36.
8. G.K. Low, G.E. Batley, *J. Chromat.*, 1987, **392**, 193.
9. R. Rajagopalan, *et. al.*, *Sci. Total Environm.* 1983, **27**, 1.
10. A. Labudzinska, *et. al.*, *ICRI Annual Report*, 1993. p. 84.

	Softening Point (°C)	Dropping Point (°C)	Penetration ($\times 10^{-4}$ m, 50°C)	Toluene Insolubles (% w/w)	BAP Content (% w/w)
Original Pitch	68.5	82.0	8.3 \pm 1.5	17.20	1.83 ***
Pitch after 6 h of heating without removal of distillate at (°C)					
150	72.0	85.5	9.3 \pm 1.4	18.04	1.81
250	76.0	88.0	4.5 \pm 1.1	19.98	1.82
300	75.0	87.5	5.3 \pm 0.5	20.50	1.77
350	77.0	88.0	5.3 \pm 0.6	23.68	1.79
380 *	83.0	97.0	1.3 \pm 0.5	27.84	1.71
Pitch after 6 h of heating with distillate removal at (°C)					
350 - 400	88.0	102.5	—	32.20	1.64 **
400 - 430	111.0	130.0	—	52.59	1.48 **

Table I. Properties of thermally treated coal-tar pitch.

* 4 h.

** in terms of 100 g of pitch.

*** distributed into acetone-solubles (1.72%), acetone-insolubles (0.08%), and toluene-insolubles (0.03%).

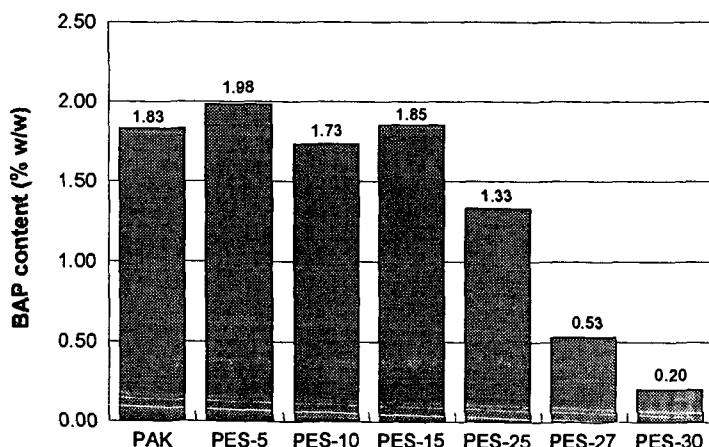


Fig. 1. Benzo(a)pyrene content in coal-tar pitch modified by polyesters. PES-5 relates to a composition of coal-tar pitch containing 5% w/w polyester resin.

THE PRODUCTION OF CHARs BY SUPERCRITICAL FLUID EXTRACTION

Edwin S. Olson and Ramesh K. Sharma
University of North Dakota
Energy & Environmental Research Center
PO Box 9018
Grand Forks, ND 58202-9018
(701) 777-5000

Key Words: Supercritical fluid extraction; SFE; char

ABSTRACT

Novel techniques were explored for developing larger micropore structure in the char prepared by supercritical fluid extraction of low-rank coals. Extractions were carried out with 2-butanone at various temperatures and pressures above the critical point, and experiments were performed to maintain the high-surface-area char structure as the pressure was released. The temperatures and pressures were then brought down close to the critical point, and then the pressure was released very slowly while keeping the temperature constant. This aerogel method gave higher surface areas than the method in which temperature or pressure was abruptly lowered, but ultraporous materials were not obtained. The introduction of pillaring reagents under supercritical conditions to preserve the expanded pore structure was also attempted. These experiments were again only partially successful in increasing the surface area of the char.

INTRODUCTION

Supercritical fluid extraction (SFE) of volatile material from coal offers an alternative to coal pyrolysis for production of char. Previous efforts with low-rank coals at the University of North Dakota gave char with relatively low surface areas. However, x-ray scattering experiments in an aluminum-beryllium high-pressure high-temperature extraction cell showed that very large surface areas ($>2000 \text{ m}^2/\text{g}$) are present during SFE of Wyodak subbituminous coal with an organic solvent, but the pores collapse during the reversion back to subcritical conditions (1).

New techniques were explored to attempt to maintain the ultraporous structure that develops in the low-rank coals under supercritical conditions. Following supercritical solvent extraction of some of the coal material, attempts were made to stabilize the highly porous structure so that it did not undergo the collapse normally observed when the pressure is brought back to ambient. The techniques involve careful release of pressure at the critical point of the solvent as in the preparation of aerogel precursors and introduction of a stabilizing agent under pressure with a high-pressure liquid chromatograph (HPLC) injection device. The stabilizing agents were boron, silicon, and titanium compounds that could decompose to oxide clusters which could pillar the micropore structure.

EXPERIMENTAL

Wyodak (Clovis Point) subbituminous coal, Gascoyne (Knife River) lignite, and Velve lignite were used for the supercritical extractions. These coals were ground to -60-mesh size and dried in an oven at 110°C for several hours. The samples were then stored under argon in plastic containers until used. 2-Butanone and ethanol were used as solvents. Tetraethyl orthosilicate (TEOS), titanium tetraisopropoxide (TIP), and tributyl borate (TBB) were added to the coal to stabilize the micropores generated during extraction.

An HPLC column (Supelco, 250-mm long, 8.5-mm i.d. \times 12.5-mm o.d.) was used for supercritical extraction of coal because it could withstand the high pressure and temperature (up to 2500 psi and 350°C , respectively). The supercritical fluids (2-butanone or ethanol) were introduced into the stainless steel reactor via an ISCO LC-5000 syringe pump (ISCO, Lincoln, NE, USA), an injector (Rheodyne, Cotati, CA, USA), and a 2-m long (1/16-in.-o.d. \times 0.02-in.-i.d.) stainless steel preheating coil. The reactor and the preheating coil were placed inside a gas chromatograph (GC) oven (Varian, Aerograph series 1400 GC) to control the extraction temperature. A fluid flow rate of approximately 1-2 mL/min (measured at the pump) was achieved using a needle valve and a 1-m \times 0.1-mm silica capillary restrictor attached to the outlet of the extraction tube.

The reactor was packed with 5 g of desired coal and placed in the oven. After the extraction apparatus was assembled, the reactor was filled with 5 mL of the solvent under static conditions (no flow out of the cell) while the oven was heated to desired temperature. The dynamic extraction (constant fluid flow) was then started and was continued for the desired time period. The extract was collected in an Erlenmeyer flask placed in a hood. At the end of the extraction, solvent flow was stopped, and residual solvent in the reactor was slowly released (requiring about 10 min.). Thereafter, the oven was cooled to ambient temperature, and the reactor was detached from the extraction line. The residue from the reactor was collected, dried at 110°C , weighed, and analyzed for surface area using American Society for Testing

and Materials (ASTM)-D4607 (iodine number) and by the percent iodine sorption method used by Sutcliffe Corp.

RESULTS AND DISCUSSION

Effects of Process Variables

Supercritical extraction of Wyodak coal with 2-butanone at 350°C (980 psi) for 5 min followed by extraction at 265°C for 25 min (640 psi) gave a char with a relatively low iodine number (IN) of 177 mg/g, when the temperature and pressure were dropped to ambient immediately after the extraction time. This value is just a little higher than that of the original coal (162), and indicates that the pores collapse rather quickly as a result of capillary movement of metaplast material, even at this relatively low temperature. Only 10% of the coal was extracted or volatilized in the experiment. The experiment performed under similar conditions, but with a very slow pressure release at constant temperature (265°C), gave a char with significantly higher area (IN = 243), although the amount of material extracted was about the same (8%). Further improvements in the surface area were obtained by increasing the initial extraction period at 350°C to 20 and 40 min before dropping the temperature and pressure to 265°C and 640 psi. By maintaining the temperature while slowly releasing the pressure, chars with INs of 267 and 309, respectively, were obtained, and extraction yields of 12% for both runs were obtained. The 30-min extraction at 350°C (1000 psi) followed by slow pressure release at 265°C gave a char with an intermediate surface area (IN = 283) and the same yield of 12%. Thus, the surface area appears to be directly related to the extraction time at 350°C, but the time at 265°C prior to slow pressure reduction may not be important. At a somewhat higher pressure (1250 psi) and higher solvent flow rate (2 mL/min), the 350°C, 30-min experiment gave a higher extraction (16%), but a lower area (IN = 254) was obtained. Although SFE yields are usually greater at the higher pressures (1), the surface area generated in the char is not directly related to the extract yield.

Experiments conducted with Gascoyne lignite gave chars with generally higher surface areas than those from the Wyodak subbituminous coal. When Gascoyne was extracted for 30 min at 350°C and subjected to rapidly decreasing temperature and pressure, the resulting char had an IN of 256. The corresponding experiment at 350°C (1250 psi) with slow pressure release gave a char with the IN = 361 and a similar extraction yield (12%). Increasing the pressure during the extraction (2500 psi) gave a higher extraction as expected (19%), and the IN of the char was again lower (301).

Another solvent, ethanol, was also investigated. Extraction with ethanol at 350°C (1500 psi) with slow pressure release gave a low extraction (8%) and a low surface area (IN = 137). Previous work demonstrated that the char surface is highly alkylated during SFE in alcohol (2). The alkylated metaplast may have a lower viscosity and undergo more extensive collapse.

A trial with the high-calcium Velva lignite gave a lower-area char (IN = 323) than the Gascoyne lignite under similar conditions (350°C, 1250 psi), although a higher extraction yield was obtained (25%). This could be attributed to increased solubility of the decomposing coal materials (metaplast) because of calcium-catalyzed decarboxylation. Normally, only partial decarboxylation occurs at 350°C.

Effects of Pillaring Additives

To stabilize the high surface areas that develop during SFE, solutions of various alkoxides were introduced under supercritical conditions following the extraction. It was anticipated that the alkoxides would decompose on the coal surface to form metal oxide clusters that would serve as stabilizing pillars to keep the pores from collapsing. Three of these organometallic agents were investigated for their effects in modifying the porosity of the supercritical chars.

Addition of TEOS to char produced by SFE of Wyodak coal at 350°C for 5 min (1050 psi) gave a modified char with a higher surface area (IN = 293) than that produced without the TEOS (IN = 243). Titanium isopropoxide addition under the same conditions gave a slightly lower area char (IN = 238). Addition of TEOS to the char obtained by extraction of Wyodak at 350°C for 20 min also gave a modified char with higher area (IN = 281), but this showed less of an increase. When less TEOS (1/3 of the previous amounts) was added to the 20-min SFE char, the increase in area was greater (IN = 297). When TEOS and TIP were added to Wyodak extracted for 30 min, the INs were similar to those for the 20-min runs. Addition of TBB to the 30-min char gave a significantly higher area char (IN = 328).

Similar experiments with Gascoyne lignite were inexplicably not effective in promoting the surface area and, instead, decreased it substantially. Tributyl borate gave a char with IN = 266, compared with the original at IN = 361. Addition of a thiol to capture radicals generated during thermal reactions of the coal also gave a low-area char.

The chars produced by this treatment still contain substantial amounts of coal "volatile" material that can be released by further heating at higher temperatures. Devolatilization of the supercritical chars at 750°C and 30 min gave carbons with very low surface areas, however.

CONCLUSIONS

Several modified chars were prepared by SFE of low-rank coals to develop a large micropore structure. Pressure was released slowly at the supercritical temperature to maintain a more porous structure. Tetraethylorthosilicate, titanium isopropoxide, and tributyl borate were introduced under the supercritical conditions to attempt to stabilize the micropore structure by forming pillaring clusters.

ACKNOWLEDGMENTS

The support of the U.S. Department of Energy is gratefully acknowledged.

REFERENCES

1. Olson, E.S.; Diehl, J.W.; Horne, D.K.; Bale, H.D. *Prepr. Pap.—Am. Chem. Soc., Div. Fuel Chem.* **1988**, *33*, 826.
2. Olson, E.S.; Swanson, M.L.; Olson, S.H.; Diehl, J.W. *Prepr. Pap.—Am. Chem. Soc., Div. Fuel Chem.* **1986**, *31*, 64.

Table 1. Extractions of Wyodak

Coal	Yield, % ¹	Solvent	Reaction Conditions				PD ²	IN
			Flow, mL/min	Temp., °C	Time, min	Pressure, psi		
Wyodak	10	2-Bu ³	1	350	5	980	Fast	177
				265	25	640		
Wyodak	8	2-Bu	1	350	5	920	Slow	243
				265	25	620		
Wyodak	12	2-Bu	1	350	20	980	Slow	267
				365	10	630		
Wyodak	12	2-Bu	1	350	40	1000	Slow	309
				365	20	640		
Wyodak	16.2	2-Bu	2	350	30	1250	Slow	254
Wyodak	8	EtOH ⁴	1	246	30	1000	Fast	137

¹ Extraction wt. coal (mf) - wt. char (mf)/wt. coal (mf) × 100. mf refers to moisture free.

² Pressure drop.

³ 2-Butanone.

⁴ Ethanol.

Table 2. Extractions of Gascoyne

Coal	Yield, % ¹	Solvent	Reaction Conditions				PD ²	IN
			Flow, mL/min	Temp., °C	Time, min	Pressure, psi		
Gascoyne	13.5	2-Bu ³	1	350	30	1250	Fast	256
Gascoyne	13.2	EtOH ⁴	1	350	30	1500	Slow	280
Gascoyne	11.6	2-Bu	1	350	30	1250	Slow	361
Gascoyne	19.3	2-Bu	1	350	30	2500	Slow	301

¹ Extraction wt. coal (mf) - wt. char (mf)/wt. coal (mf) × 100. mf refers to moisture free.

² Pressure drop.

³ 2-Butanone.

⁴ Ethanol.

Table 3. Extractions of Wyodak with Stabilizer Addition¹

Coal	Yield, %	Conditions				IN
		Temp., °C	Time, min	Pressure, psi	Additive (μL)	
Wyodak	8	350	5	920	None	243
		265	25	620		
Wyodak	13.4	350	5	1050	TEOS (300)	293
		265	25	620		
Wyodak	8	350	5	920	TIP (300)	238
		265	25	650		
Wyodak	12	350	20	980	None	267
		265	10	630		
Wyodak	12	350	20	1000	TEOS (300)	281
		265	10	620		
Wyodak	12	350	20	980	TEOS (300)	297
		265	10	640		
Wyodak	12.5	350	30	1000	None	283
Wyodak	13	350	30	1000	TEOS	299
				500		
Wyodak	13.8	350	300	1200	TIP	281
Wyodak	9	350	30	1250	TBB	328

¹ Solvent = 2-butanone, flow rate = 1 mL/min, pressure drop = slow.

Table 4. Extractions of Gascoyne with Stabilizer Added¹

Coal	Extraction, %	Reaction Conditions				IN
		Temp., °C	Time, min	Pressure, psi	Additive (μL)	
Gascoyne	11.6	350	30	1250	None	361
Gascoyne	14.4	350	30	1250	TBB (300)	266
Gascoyne	10.2	350	30	1250	<i>p</i> -Thiocresol (300)	259

¹ Solvent = methylethyl ketone, flow rate = 1 mL/min.

STRUCTURAL AND THERMAL BEHAVIOR OF COAL COMBUSTION AND GASIFICATION BY-PRODUCTS: SEM, FTIR, DSC, and DTA Measurements

P. S. Valimbe¹, V. M. Malhotra¹, and D. D. Banerjee².

1. Department of Physics, Southern Illinois University, Carbondale, Illinois 62901-4401

2. Illinois Clean Coal Institute, Carterville, Illinois 62918-0008.

Keywords: Coal combustion residues, scrubber sludge, thermal and spectroscopic characterization

ABSTRACT

The pulverized coal combustion fly ash, fluidized bed combustion fly ash, fluidized bed combustion spent bed ash, and scrubber sludge samples were systematically characterized using scanning electron microscopy (SEM), differential scanning calorimetry (DSC), differential thermal analysis (DTA), and transmission Fourier transform infrared (FTIR) techniques. Our spectroscopic results indicated that the scrubber sludge is mainly composed of a gypsum-like phase whose lattice structure does not exactly match either conventional gypsum ($\text{CaSO}_4 \cdot 2\text{H}_2\text{O}$) or hanebachite ($\text{CaSO}_3 \cdot 0.5\text{H}_2\text{O}$). SEM images suggested that unlike PCC fly ash particles, which were mainly spherical, the FBC fly ash and FBC spent bed ash particles were irregularly shaped and showed considerable fusion. FBC fly ashes were mainly composed of anhydrite, lime, portlandite, calcite, hematite, magnetite, and various glass phases. The DTA and DSC data presented evidence implying that the PCC fly ash is thermally stable at $30^\circ\text{C} < T < 1100^\circ\text{C}$. However, this was not the case for FBC ashes.

INTRODUCTION

More than 800 million tons of coal per year are burned in the United States, producing approximately 10 % of the coal burned as combustion residues in the form of solids. These solids, which are largely noncombustible, are classified as "fly ash" and "bottom ash". The fly ash particles are fine materials which are mostly captured in precipitators and in bag houses. The bottom ash term is used for those materials which settle or flow as melt to the bottom of the boiler. If the boiler is designed to use pulverized coal, then the coal combustion by-products are called "pulverized coal combustion" (PCC) fly ash and PCC bottom ash.

The midwestern USA coals are high in sulfur content. The sulfur in coal is in the form of inorganic minerals (chiefly pyrite) and is also organically bound. Therefore, environmental concerns require that the sulfur content of the coal be reduced if this abundant resource is to be continuously utilized. A two prong approach is being developed to mitigate the sulfur problem. In the first, physical, chemical, and microbiological coal cleaning techniques have been and are being developed to reduce the sulfur content of midwestern coals. In the second, technologies have been developed and are being perfected to capture sulfur-containing combustion gases during coal combustion. One such clean coal technology is fluidized bed combustion (FBC)^{1,2}. The advantage of the FBC technology is that it affords a large reduction of SO_2 from the combustion gases. The sorbents, like calcium carbonate (CaCO_3) and calcium oxide (CaO), are injected along with the coal into FBC combustor. As SO_2 is produced, it reacts with the sorbent and is captured in the form of anhydrous calcium sulfate (CaSO_4)^{1,3}. There are also reports in the literature which suggest the formation of sulfides⁴. Just like for conventional combustors, two types of solid residues are produced, e.g., FBC fly ash, which leaves the combustor at the top, and FBC spent bed ash, which is left at the bottom of the combustor.

Wet scrubber processes are extensively used in flue gas desulfurization (FGD) technology. The major waste products produced are gypsum, calcium sulfite (CaSO_3), fly ash, and excess reagents⁵. Calcium sulfite may be oxidized to calcium sulfate which in combination with water forms gypsum. It is generally believed that the calcium sulfate purity of residues from wet scrubber technology using lime or limestone ranges between 95 % to 99 %.

It is estimated that by the turn of century about 200 million tons of coal combustion residue will be produced annually. With the current cost of residue disposal expected to rapidly escalate, the economic stakes for the coal utilization industry are substantial. Consequently, the technologies which can convert combustion residues into high value, but economically sound, materials are of utmost importance. Presently, only about 25% of the combustion residues generated are utilized⁶, with the rest going to landfill or surface impoundments. Therefore, efforts are underway to find alternative usage^{6,9} of the combustion residues, e.g., ultra-lightweight aggregates for insulation industry, Portland cement-based FBC mixes, highway and street construction, construction bricks or tiles, roofing or paving tiles, pipe construction, and ashalloys. We have recently initiated research in our laboratory in which we are attempting to form advanced composite materials from coal combustion residues obtained from Illinois utilities. However, the successful utilization of coal

combustion and gasification residues requires a thorough physical and chemical characterization of these ashes.

EXPERIMENTAL TECHNIQUES

For our characterization studies, we examined four samples, i.e., PCC fly ash (Baldwin), FBC fly ash (ADM), FBC spent bed ash (ADM), and scrubber sludge (CWLP). The residue samples were obtained from the sample bank established at the Mining Engineering Department of Southern Illinois University at Carbondale. The magnetic content of PCC fly ash, FBC fly ash, and FBC spent bed ash was extracted from the as-received ashes by applying a magnetic separation technique.

Microscopic studies of the coal combustion residues were accomplished using a Hitachi S570 scanning electron microscope. The samples were mounted on the SEM sample stubs using sticky tabs. The mounted samples were then cured at 60°C for 24 hours to ensure that the ash particles would not detach from the stub while under the electron beam. After curing, the samples were sputter coated with 40 nm of gold layer to help eliminate the problem of sample charging. The SEM data were collected using an accelerating voltage of 20 kV, except for FBC spent bed ash whose SEM pictures were acquired at an accelerating voltage of 10 kV to reduce sample charging.

The structural characteristics of the combustion ashes and scrubber sludge were probed by recording their FTIR spectra. We used KBr pellet technique to collect the infrared spectra on a IBM IR44 FTIR spectrometer. One hundred scans were acquired at a 4 cm⁻¹ resolution. Since the as-received scrubber sludge sample was wet, i.e., had substantial amount of moisture in it, the sludge was dried at 100°C prior to making its KBr pellets.

The thermal behavior of coal combustion residues and scrubber sludge were obtained using DSC and DTA techniques. The DSC data were recorded on PCC fly ash, FBC fly ash, FBC spent bed ash, and scrubber sludge using a well calibrated¹⁰⁻¹² Perkin-Elmer DSC7 system interfaced with a 486 PC computer. The procedures adopted for the calibration of the temperature and of the specific heat have been described elsewhere¹². Our calibrated DSC system had a temperature precision of ± 1 K. The thermal characteristics of the residues using DSC technique were ascertained at 30°C < T < 600°C. We used a heating rate of 20°C/min under a controlled N₂ purge environment (30 cm³/min) to collect our DSC data.

The thermal stability of fly ashes, spent bed ash and scrubber sludge at 50°C < T < 1010° was examined by acquiring DTA data using a Perkin-Elmer DTA7 system. The samples were heated from 50°C to 1000°C under a nitrogen gas environment. The heating rate used was 20°C/min.

RESULTS AND DISCUSSION

Microscopic Studies: Figures 1, 2, 3, and 4 reproduce the SEM micrographs of PCC fly ash, FBC fly ash, FBC spent bed ash, and scrubber sludge, respectively. The PCC fly ash particles were mainly composed of spherically-shaped particles whose sizes ranged from 0.2 mm to 15 mm. The spherical particles were usually hollow. It should be noted from Fig. 1 that small spherical particles of PCC fly ash were attached to bigger fly ash particles giving the appearance of agglomerates. Our SEM data on PCC fly ash did show some irregularly shaped particles in the ash, but predominantly particles were spherical. From the SEM micrographs of FBC fly ash, it appears that this ash had small particles of the range 0.1 mm to 1 mm, which had fused together to form agglomerates of the size ranging from 2 mm to 100 mm. Our SEM micrographs also indicated that the FBC fly ash contained very little spherical particles unlike PCC fly ash. The lack of the presence of spherical particles in FBC fly ash may be due to the lower combustion temperatures¹⁻² for FBC combustor (around 850°C) than for PCC combustor (around 1150°C). The microscopic analysis of the FBC spent bed ash exhibited three distinct types of particles in this ash material. The first type of particles had a smooth surface to which smaller particles (i.e., 2 mm - 10 mm) were fused. These smooth particles lacked any pore structure. The second type of particles showed varying shapes and sizes but generally was around 750 mm. The third type of particles in this ash had a glass-like structure. These particles had an extensive pore structure, as can be seen in Fig. 3, and their sizes ranged from 250 mm - 300 mm. Figure 4 reproduces the SEM micrographs of scrubber sludge particles which were dried at room temperature. Generally, the sludge particles had a whisker-like shape, ranging from 50 mm to 400 mm in length, and were about 50 mm thick. In addition to the whisker-like particles, the sludge had some agglomerated particles whose average size was about 100 mm.

Thermal Behavior: The thermal stability of the PCC fly ash, FBC fly ash, FBC spent bed ash, and scrubber sludge was probed by recording their DSC and DTA data. The main thermal events observed from our DSC results are summarized in Table 1. The high temperature thermal stability of the combustion residues was ascertained by collecting DTA data at 50°C - 1000°C. We summarize our DTA results in Table 2, and Fig. 5 depicts typical DTA curves obtained from the combustion residues and scrubber sludge. The thermal data can be summarized as follows: (a) The PCC fly ash

contained moisture which was evolved on heating the ash at 155°C and 185°C. Besides these two minor endothermic reactions, the DTA curve of PCC fly ash depicted an additional weak endothermic peak at 574°C. It is well known¹³ that β -quartz undergoes transformation to α -quartz at 573°C. Therefore, the weak endotherm observed at 574°C for the PCC fly ash could be assigned to the presence of quartz in the ash. Our PCC fly ash sample, besides minor endothermic reactions at 155, 185, and 574°C, remained thermally inert up to 1000°C, thus making it an excellent raw material for the fabrication of composite materials. (b) It should be noted from Tables 1 and 2 that the FBC fly ash and FBC spent bed ash appeared to have similar thermal behaviors, i.e., thermal decomposition reaction at ~438°C which could be associated with the decomposition¹⁴ of $\text{Ca}(\text{OH})_2$ into CaO and H_2O . The presence of $\text{Ca}(\text{OH})_2$ in the FBC fly ash and FBC spent bed ash was not entirely surprising notwithstanding that these ashes were subjected to combustion temperatures of around 850°C. The probable source of $\text{Ca}(\text{OH})_2$ in our ashes could be moisture's reaction with CaO during the storage of ash material.

TABLE 1
Summary of the Thermal Events of the Combustion Residues as Determined by DSC at
 $30^\circ\text{C} < T < 590^\circ\text{C}$.

Sample	Thermal Event	Temperature (°C)	% Weight Loss on Heating the sample to 580°C
PCC Fly Ash	-	-	4.4
FBC Fly Ash	Endothermic	420	2.7
FBC Spent Bed Ash	Endothermic	420	1
Scrubber Sludge	Endothermic	141	17.2
	Endothermic	176	
	Exothermic	380	

The additional endothermic event at 674°C for FBC fly ash strongly suggested the presence of hematite ($\alpha\text{-Fe}_2\text{O}_3$) in this ash. It should be noted from Fig. 5 that this thermal event was absent from the spent bed ash's DTA curve. The weak endothermic peak could be assigned to the magnetic transformation of hematite¹³. (c) The DSC and DTA curves for the scrubber sludge showed a strong endothermic peak at 180°C and a weak exothermic peak at 380°C. The endothermic peak at 180°C suggested the dehydration of the gypsum, i.e.,



From their thermogravimetric experiments, Dorsey and Buecker¹⁵ suggested the presence of calcium sulfite in their sample of scrubber sludge. They reported weight loss at $408^\circ\text{C} < T < 452^\circ\text{C}$ from their sample and associated this weight loss with the dehydration of hemihydrate ($\text{CaSO}_3 \cdot \text{CaSO}_4 \cdot 1/2\text{H}_2\text{O}$), i.e.,



As listed in Table 2, the exothermic peak at 380°C for our scrubber sludge sample began at around 348°C and terminated at around 493°C. Therefore, one may argue that the exothermic peak at 380°C could be assigned to the dehydration of hemihydrate. The FTIR spectrum of our scrubber sludge sample did not show any oscillators at 970 and 945 cm^{-1} due to sulfite ions. Moreover, dehydration should produce an endothermic peak. It has been reported in the literature¹⁶ that on heating gypsum it undergoes a polymorphous transformation at $370^\circ\text{C} < T < 460^\circ\text{C}$ which results in a weak, exothermic peak. Therefore, we assigned the exothermic peak at 380°C for our scrubber sludge to this polymorphous transition.

Spectroscopic Characterization: The spectroscopic studies of various combustion residues were undertaken to characterize the mineral and glass phases of the PCC fly ash, FBC fly ash, FBC spent bed ash, and scrubber sludge. In Fig. 7 we have reproduced the transmission-FTIR spectrum of scrubber sludge particles which were air dried prior to recording their spectrum. Three very strong bands were observed at 1154, 1126, and 1105 cm^{-1} . In addition, a doublet having frequencies 662 and 602 cm^{-1} was observed. In the water's stretching region, two distinct vibrational modes could be seen at 3617 and 3559 cm^{-1} . In the water's bending region only a single oscillator was observed at

1620 cm^{-1} . It is generally believed that the FGD residue, e.g., scrubber sludge, contains calcite (CaCO_3), hannebachite ($\text{CaSO}_4 \cdot 0.5\text{H}_2\text{O}$), gypsum ($\text{CaSO}_4 \cdot 2\text{H}_2\text{O}$), quartz (SiO_2), and troilite (FeS). The absence of any vibrational bands below 450 cm^{-1} led us to discount the presence of troilite in our sample. Since we did not observe any band in the FTIR spectrum of the scrubber sludge at around 1430 cm^{-1} , we could also rule out the presence of calcite particles in our sludge sample. The argument that quartz may be present in our sample was discarded because the diagnostic bands for it at around 1050 and 472 cm^{-1} were not observed in our FTIR spectrum. However, our transmission-FTIR data did suggest the presence of gypsum. The vibrational bands at 1154, 1126, and 1105 cm^{-1} could be assigned to ν_3 of sulfate of gypsum, while the oscillators at 662 and 602 cm^{-1} could be attributed to ν_4 of sulfate ions. The presence of two vibrational modes in the water's stretching region implied that there are two types of hydrates in our scrubber sludge. A comparison of a commercially available gypsum's FTIR spectrum, see Fig. 7, with our scrubber sludge spectrum indicated that gypsum formed in the FGD residue had a lattice structure which was different from that of commercial gypsum. It is worth pointing out that the FTIR spectrum of bassanite ($\text{CaSO}_4 \cdot 0.5\text{H}_2\text{O}$) shows a vibrational mode at about 3615 cm^{-1} and we observed a band at 3617 cm^{-1} . However, we could not assign 3617 cm^{-1} band to bassanite because the accompanying water band at 3465 cm^{-1} was absent in our spectrum. We also ruled out the presence of hannebachite because of two reasons, i.e., (a) we did not observe the expected strong bands at 975 and 940 cm^{-1} of SO_4 ion in our FTIR spectrum of the scrubber sludge, and (b) we did not see any rectangular crystals, which could be associated with hannebachite, in our SEM images of the sludge. In

TABLE 2
The Thermal Characteristics of the Combustion Residues as determined by DTA
at $50^\circ\text{C} < T < 1100^\circ\text{C}$.

Sample	Peak Begins ($^\circ\text{C}$)	Peak Ends ($^\circ\text{C}$)	Peak Temperature ($^\circ\text{C}$)
PCC Fly Ash			155
	460	701	185
			574
FBC Fly Ash	348	542	438
	615	729	674
FBC Spent Bed Ash	190	245	205
	344	491	442
Scrubber Sludge	96	275	180
	348	493	380

view of the discussion presented above we argue that scrubber sludge is mainly composed of gypsum. However, its lattice structure is not identical to the lattice structure of conventional gypsum.

The transmission-FTIR spectrum of PCC fly ash, FBC fly ash, and FBC spent bed ash is reproduced in Fig. 7, and the observed frequencies are listed in Table 3. Based on the observed FTIR spectrum, it is argued that PCC fly ash is largely composed of various oxides. The strongest bands in our transmission-FTIR spectrum of PCC fly ash originated from quartz. The transmission-FTIR spectrum of as-received FBC fly suggested the presence of quartz, anhydrite (CaSO_4), lime (CaO), portlandite (Ca(OH)_2), calcite, hematite (Fe_2O_3), magnetite (Fe_3O_4), and glass phases. From the observed infrared frequencies of FBC spent bed ash, which are listed in Table 3, the following minerals have been identified, i.e., anhydrite, lime, portlandite, calcite, periclase, hematite, and magnetite. It is also generally reported that spent bed ash contains CaS. The formation of CaS is believed to occur for circulating fluidized bed combustion (FBC) via the following reaction, i.e., $\text{CaO} + \text{H}_2\text{S} \rightarrow \text{CaS} + \text{H}_2\text{O}$. However, it is difficult for us to confirm the presence of CaS in our FBC spent bed ash as CaS produces no infrared bands.

ACKNOWLEDGMENTS

This research was supported by grants made possible by the U. S. Department of Energy Cooperative Agreement Number DE-FC22-92PC92521 and the Illinois Department of Energy through the Illinois Coal Development Board and the Illinois Clean Coal Institute. Neither the authors nor the U. S. Department of Energy, Illinois Clean Coal Institute, nor any person acting on behalf of either: (A) Make any warranty of representation, express or implied, with respect to the accuracy, completeness, or usefulness of the information contained in this report, or that the use of

any information, apparatus, method, or process disclosed in this report may not infringe privately-owned rights; or (B) Assume any liabilities with respect to the use of, or for damages resulting from the use of, any information, apparatus, method or process disclosed in this report. References herein to any specific commercial product, process, or service by trade name, trademark, manufacturer, or otherwise, does not necessarily constitute or imply its endorsement, recommendation, or favoring by the U. S. Department of Energy. The views and opinions of authors expressed herein do not necessarily state or reflect those of the U. S. Department of Energy.

REFERENCES

1. M. Valk, "Fluidized Bed Combustors" in 'Fluidized Bed Combustion', M. Radovanovic, Ed., Hemisphere Publishing Co., Washington (1986).
2. L. Yaverbaum, 'Fluidized Bed Combustion of Coal and Waste Materials', Noyes Data Co. (1977).
3. R. J. Collins, J. Testing and Evaluation **8**, 259 (1980).
4. E. E. Berry, R. T. Hemmings, B. J. Cornelius, and E. J. Anthony, "Sulphur Oxidation States in Residues From a Small-Scale Circulating Fluidized Bed Combustor" in 'Fly Ash and Coal Conversion By-Products Characterization, Utilization and Disposal V', R. T. Hemmings, E. E. Berry, G. J. McCarthy, and F. P. Glasser, Eds., Materials Res. Soc. Proc. **136**, 9 (1989).
5. L. B. Clarke, "Management of FGD Residues: An International Overview", Procd. 10th Annual Inter. Pittsburgh Coal Conf., S-H Chiang, Ed., pp 561-566 (1993).
6. D. Golden, EPRI Journal, January/February, pp 46-49 (1994).
7. C. A. Holley, Preprints, Am. Chem. Soc. Fuel Div. **36(4)**, 1761 (1991).
8. O. P. Modi, A. K. Singh, A. H. Yegneswaran, and P. K. Rohatgi, J. Materials Science lett. **11**, 1466 (1992).
9. S. Ciby, B. C. Pai, K. G. Satyanarayana, V. K. Vaidyan, and P. K. Rohatgi, J. Materials Eng Performance **2**, 353 (1993).
10. S. Jasty, P. D. Robinson, and V. M. Malhotra, Phys. Rev. B **43**, 13215 (1991).
11. R. Mu, and V. M. Malhotra, Phys. Rev. B **44**, 4296 (1991).
12. S. Jasty, and V. M. Malhotra, Phys. Rev. B **45**, 1 (1992).
13. R. C. Mackenzie and G. Berggren in 'Differential Thermal Analysis. Volume 1: Fundamental Aspects', R. C. Mackenzie, Ed., Academic Press, New York (1970).
14. O. Chaix-Plucher, J. C. Niepce, and G. Martinez, J. Materials Sci. Lett. **6**, 1231 (1987).
15. D. L. Dorsey and D. Buecker, Res. & Develop., May (1986).
16. D. N. Todor, 'Thermal Analysis of Minerals', Abacus Press, Kent (1976)

TABLE 3

This table summarizes the observed infrared bands for PCC fly ash, FBC fly ash, and FBC spent bed ash. The observed frequencies are in cm^{-1} .

PCC Fly Ash	FBC Fly Ash	FBC Spent Bed Ash	Comments	Assignment
3,642	3,642	3,642	sharp	O-H stretch $[\text{Ca}(\text{OH})_2]$
3,448	3,462	3,448	broad	O-H stretch, adsorbed water
1,631		1,624	sharp, weak	H-O-H bend of water
	1,449	1,448	broad, medium	asymmetric CO_3^{2-} stretch $[\text{CaCO}_3]$
	1144	1154	broad, strong	SO_4^{2-} stretch
	1111	1122	broad, strong	$[\text{CaSO}_4]$
1,072	1,011		broad, strong	Si-O stretch
		945	broad, weak	CaSO_3
	885	920	sharp, weak	O-H bend $[\text{Ca}(\text{OH})_2]$
			sharp, weak	CaCO_3
794	795		sharp, medium	quartz
778			sharp, weak	quartz
694			sharp, weak	quartz
	681	680	sharp, weak	Anhydrite $[\text{CaSO}_4]$
613	616	615	sharp, weak	Anhydrite $[\text{CaSO}_4]$
	602	605	sharp, weak	Anhydrite $[\text{CaSO}_4]$
593		595	sharp, weak	Anhydrite $[\text{CaSO}_4]$
560		560	broad, weak	Fe_2O_3 and Fe_3O_4
	515		broad, weak	oxides
462	462	462	broad, medium	quartz

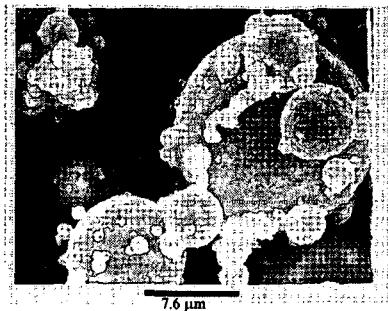


Figure 1. SEM photo of PCC fly ash showing the spherical nature of the particles.

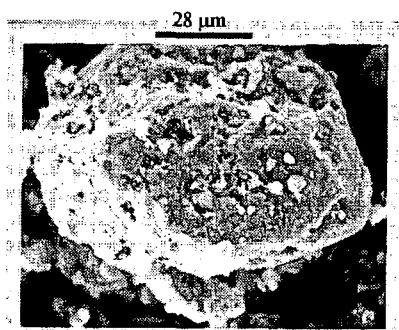


Figure 2. SEM photo of FBC fly ash.

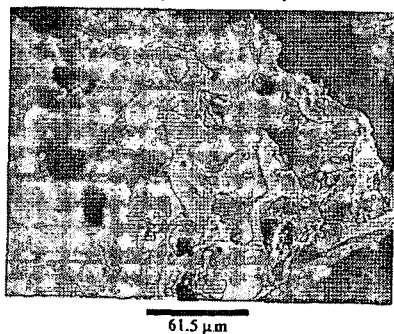


Figure 3. SEM photo of FBC spent bed ash.

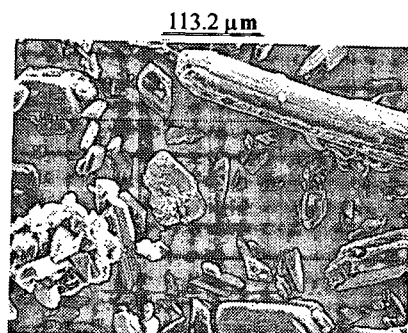


Figure 4. SEM photo of scrubber Sludge

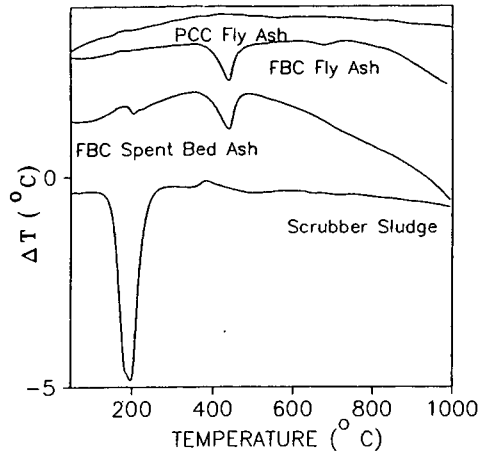


Figure 5. Differential thermal analysis (DTA) of combustion residues and scrubber sludge.

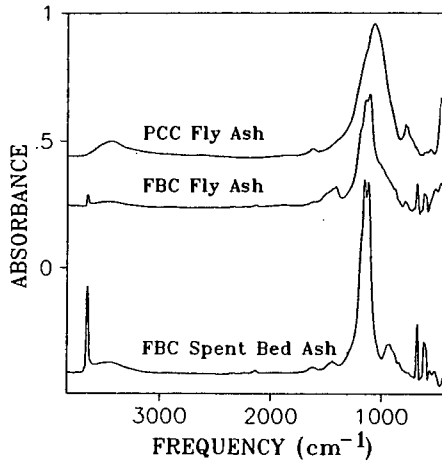


Figure 6. FTIR spectrum of combustion residues.

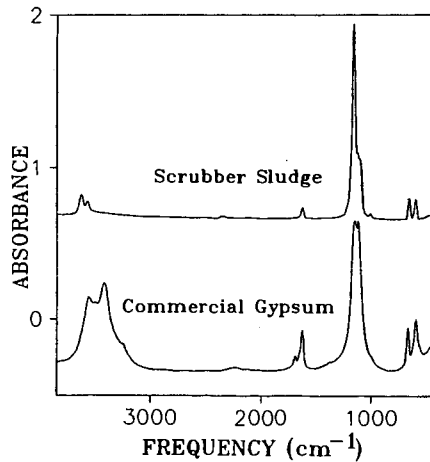


Figure 7. FTIR Spectrum of scrubber sludge and a commercial gypsum sample.

A COMPARISON OF ZEOLITE AND DOLOMITE AS GASIFICATION TAR-CRACKING CATALYSTS

Ronald C. Timpe and Brian C. Young
Energy & Environmental Research Center
University of North Dakota
Grand Forks, ND 58202-9018

Keywords: tar-cracking catalysts, gasification, zeolite, dolomite

ABSTRACT

Unconverted liquid products produced during steam gasification of coal are heavy tars. The object of this study was to compare a zeolite with dolomite as tar-cracking catalysts. Up to 75% of the tars from a lignite and a subbituminous coal were cracked to lower molecular weight compounds by use of a heated catalyst bed. Collection of the tars downstream of the catalyst bed resulted in approximately 50% less tar from the test with dolomite as the catalyst than with zeolite. Simulated distillations of the tars showed more effective cracking with the dolomite than with the zeolite.

INTRODUCTION

Tar produced in the gasification of coal is deleterious to the operation of downstream equipment, including fuel cells, gas turbines, hot-gas stream cleanup filters, and pressure-swing adsorption systems. Catalytic cracking of tars to smaller hydrocarbons can be an effective means of removing these tars from gas streams and, in the process, generating useful products, e.g., methane gas, which is crucial to operation of molten carbonate fuel cells.

The need for on-line cracking of gasification tars is common to many processes involving gas stream cleanup. Aerosol tars are not readily removed from gas streams by conventional means and, as a consequence, often result in plugged filters or fouled fuel cells, turbines, or sorbents. Catalytic cracking of tars to molecular moieties of C_{10} or smaller would prevent these problems. As an example, the moving Bourdon (fixed-bed) gasifier by virtue of its efficient countercurrent heat exchange and widespread commercial use may offer the lowest-cost IGCC system, provided tar generation and wastewater contamination can be minimized. This study involved catalytic tar cracking to evaluate the potential of selected catalysts to minimize tar accumulation and maximize char conversion to useful liquid and/or gaseous products.

EXPERIMENTAL

Two low-rank coals (LRC) were chosen for testing the tar-cracking propensity of dolomite and a zeolite (Engelhard X-2388). The proximate analyses of the Beulah West Pit lignite and Beluga Alaskan subbituminous are shown in Table 1.

Pyrolysis and steam gasification were carried out in the integrated bench-scale gasifier (IBG). A module for containing a catalyst bed was fabricated and connected by flange to the top of the IBG reactor. The module was heated through contact with the reactor (conduction) and flow-through of gases from the reactor (convection). Operated in the fluidized mode, the fully instrumented IBG was used to pyrolyze and gasify coal. The gas and tar produced exited the reactor through the catalyst module containing a hot catalyst (dolomite or zeolite) bed, passed through two water-cooled condensers, and was analyzed by on-line Fourier Transform infrared spectrometry (FT-IR). Trapped liquids were collected in two water-cooled condensers connected in series and were saved for later analysis. In addition, the product gas was sampled periodically by collecting samples in gas bags for later analysis by gas chromatography (GC).

IBG

The IBG is a small batch process gasifier, with a charge capacity of nominally 70 g of coal. This unit provides data on the effects of bed fluidization, conversion of feedstock, reaction rate response to temperature, pressure, catalyst and feed gas composition and flow rate, and gaseous products, while providing sufficient quantities of conversion products for subsequent analysis. The top of the reactor has been fitted with a catalyst module through which the hot exhaust gas must pass before entering the series of two condensers. Although the module has no heaters of its own, it receives heat from the reactor and tends to remain predictably within 50°–100°C of the reactor. A typical catalyst charge to the module is 30–50 g. Gas flows uninterrupted through the system and through the heated FT-IR cell. Gas exiting the second condenser flows through the cell where it is analyzed. The data obtained indicate the effect on the tar by noting the levels of methane in the gas stream. In this study, dolomite and zeolite were tested for their effect on the pyrolysis tar.

RESULTS

Gas Production During Steam Gasification of Beulah Lignite

Table 2 shows the operating parameters for steam gasification of Beulah West Pit lignite in the IBG. The temperatures at which the Beulah lignite was gasified were selected on the basis of potential operating temperatures of various gasifiers. Beluga subbituminous coal was gasified at only one temperature, i.e., 800°C. The conversions shown are based on maf proximate analysis values for volatiles and fixed carbon in raw coal sample. There was a clear conversion trend with temperature, with 90 wt% conversion or above occurring at or above 700°C. Each reaction was carried out at the gasification temperature indicated until the production of CO₂ as monitored by IR spectrometry became negligible, generally 1 to 3 hours. The dolomite tended to decrepitate, producing fines, some of which blew over into the primary trap. The quantities of dolomite blown over did not correlate with temperature, but rather the fines tended to blow over with the occasional random increases in gas flow resulting primarily from uneven steam flow.

The methane content of the gaseous product normalized to the volatiles content of the coal from tests at each of the five gasification temperatures are shown in Figure 1. Pyrolysis methane is produced initially at temperatures above 500°C and drops off after about 25 minutes into the run. Methane continues to be produced as a result of methanation reaction and catalytic cracking. Methane is not a product of the reaction carried out at 250°C, but substantial methane is produced at each of the other temperatures. Indeed, at 700°C, more methane relative to the volatiles content was produced than at 850°C.

Tar Production During Steam Gasification of Beulah Lignite

The tar collected from each of the tests listed in Table 2 was analyzed following collection of the tar from the tubing and extraction from the liquids collected in the condensers. Table 3 shows the tar content collected following the catalyzed tar-cracking experiments (Tar_c) at each of the five temperatures, relative to the tar content collected following the uncatalyzed tar-cracking experiments (Tar_u) at each of the same temperatures. During each of these experiments, the catalyst was heated by the reactor and the flowing gases and was approximately 50°-100°C cooler than the reactor temperature shown in Table 3. Dolomite decrepitation and powder carryover contributed to the unexpectedly high dolomite tar recovery at 700°C. Care was taken following during the remaining tests to ensure that this effect was minimized. Examination of the tar recovered from the 800+°C test showed a small amount of particulate material, probably dolomite in origin. Noticeable amounts of particulates were not found in the remaining tar samples.

Characterization of the tar was by simulated distillation. This technique was carried out on a Hewlett-Packard 5890 gas chromatograph equipped with a flame ionization detector (FID). A column and a hydrogen carrier gas flow at ~1 cm³/min was used to separate the components. The temperature ramp was 2°C/min to 40°C, then 8°C/min to 320°C. The 1 µl injection was split 1:50. Peak area % was calculated from area counts exclusive of solvent peak and was used to approximate relative component concentrations. No attempt was made to identify individual components, but they were assumed to be primarily hydrocarbons.

Plots of chromatography cumulative peak area % versus retention time for simulated distillations of tars collected from the tar cracking tests with and without catalyst at the temperatures of the tests are shown as Figures 2-4. Tar produced during steam gasification at 800+°C undergoes some thermal cracking without benefit of cracking catalyst, as shown in Figure 2. Lighter organics with boiling points of approximately 150°C and 175°C constituted >50 area% of gas chromatographic components of the tar produced at 800+°C. The component distributions of the tars produced at 400°, 550°, and 700°C as determined by area% were not readily distinguishable. The lighter organics with boiling points of approximately 150° and 175°C made up approximately 40 area% of the gas chromatographic components produced at 400°, 550°, and 700°C.

The effluent gas stream passed through a dolomite bed contained few tar components that boiled in the range 200° to 375°C, as shown by Figure 3. This compares with 25-30 area% of the tar over the same temperature range when not subjected to contact with a catalyst bed. The tars from each of the four tests with dolomitic show a large area% for components boiling at a temperature >375°C. The rest of the components have boiling points below approximately 225°C.

Tar produced at 550°C and passed through a zeolite bed at approximately 450°-500°C had approximately 55% of its organic components in the boiling point range equal to or less than 175°C, as shown by Figure 4. Tar produced at 700°C and passed through a zeolite bed at approximately 600°-650°C had greater than 60 area% representing components with boiling points of approximately 175°C or less. Tar components in the same boiling point range produced during an 800+°C gasification test and passed through a bed of zeolite at 700°-750°C were represented by less than 50 area%. Components boiling at <270°C were represented by 60 area% of the 800+°C tar plot.

Tar Production During Steam Gasification of Beluga Subbituminous Coal

The reduction in tar quantity by zeolite and dolomite tar-cracking catalysts was determined from data obtained at 800°C gasification of Beluga subbituminous coal using the IBG. Dolomite was shown to be more effective in cracking the tar than the zeolite. The bulk tar collected after cracking with zeolite was 58 gas chromatographic area% and approximately one-half the weight of the tar collected with no cracking catalyst, as compared with 28 gas chromatographic area% and approximately one-fourth the weight for cracking with dolomite. In addition, the chromatograms showed greater total components with dolomite than with zeolite.

CONCLUSIONS

- 50% or more of tar produced during steam gasification of Beulah lignite at temperatures of 400°-800 + °C is cracked by either dolomite or zeolite where the temperature of the catalyst is 50°-100°C below that of the reactor.
- Dolomite decrepitated during heating, especially at the temperatures > 550°C, resulting in loss to downstream collection devices.
- Overall, dolomite was more effective in the lignite tar cracking, but the X-2388 zeolite appeared to give slightly better results with the very heavy ends (tars) produced at the higher temperatures.

ACKNOWLEDGMENTS

The authors wish to thank the Engelhard Corporation for providing the zeolite catalyst and the U.S. Department of Energy and the Morgantown Energy Technology Center for the support to carry out this work. Thanks is also extended to Ron Kulas and Jerry Petersburg for their assistance with the laboratory and IBG work.

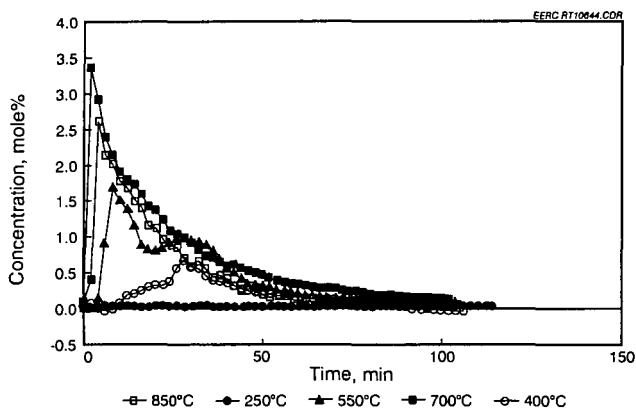


Figure 1. Methane concentration relative to tar production at each of five gasification temperatures.

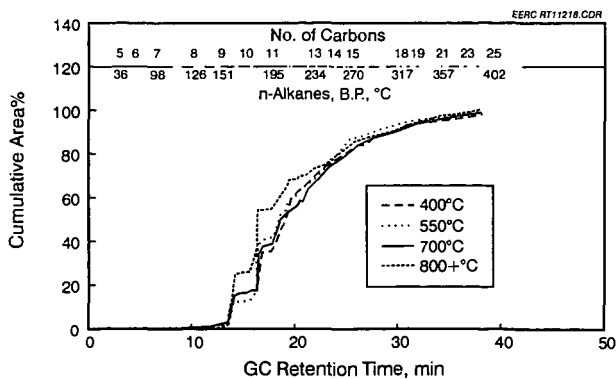


Figure 2. Simulated distillation of tar collected during gasification of Beulah lignite at 400°, 550°, 700° and 800 + °C.

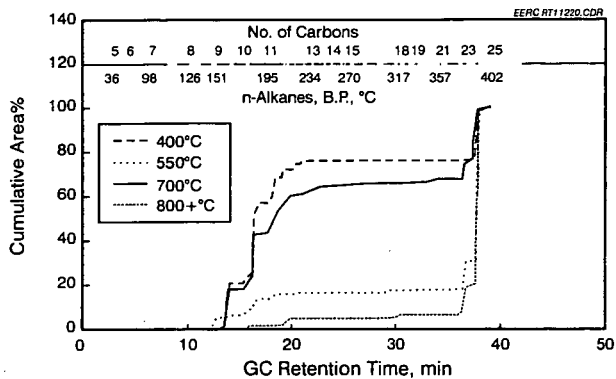


Figure 3. Simulated distillation of dolomite-cracked tar collected during gasification of Beulah lignite at 400°, 550°, 700°, and 800+°C.

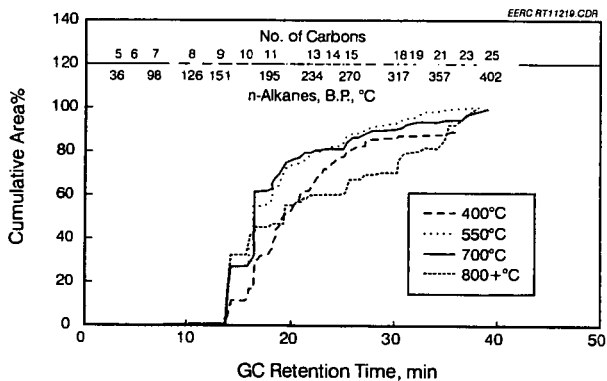


Figure 4. Simulated distillation of zeolite-cracked tar collected during gasification of Beulah lignite at 400°, 550°, 700°, and 800+°C.

TABLE 1

Proximate Analysis of Beulah West Pit Lignite and Beulah Subbituminous				
Coal	Moisture, AR, wt%	Volatiles, mf, wt%	Fixed Carbon, mf, wt%	Ash, mf, wt%
Beulah West Pit	30.2	44.8	47.6	7.6
Beluga (Alaskan)	22.3	45.0	44.5	10.5

TABLE 2

Conversion of Volatiles and Fixed Carbon to Tar and Gaseous Products
under Steam Gasification Conditions at Different Temperatures

Run No.	Coal	Temperature, °C	Catalyst	Atm., g/min at 50 psig	Conversion wt%, mf
IBG11	Beulah West	800+	Dolomite	Steam, 3-4	97
IBG11	Beulah West	250	Dolomite	Steam, 3-4	17
IBG12	Beulah West	550	Dolomite	Steam, 3-4	48
IBG12	Beulah West	700	Dolomite	Steam, 3-4	86
IBG12	Beulah West	400	Dolomite	Steam, 3-4	31
IBG12	Beulah West	250	Zeolite	Steam, 3-4	12
IBG12	Beulah West	700	Zeolite	Steam, 3-4	82
IBG12	Beulah West	700	Zeolite	Steam, 3-4	86
IBG12	Beulah West	550	Zeolite	Steam, 3-4	44
IBG12	Beulah West	800+	Zeolite	Steam, 3-4	98
IBG12	Beulah West	400	Zeolite	Steam, 3-4	34
IBG12	Beulah West	800+	None	Steam, 3-4	98
IBG13	Beulah West	250	None	Steam, 3-4	11
IBG13	Beulah West	700	None	Steam, 3-4	86
IBG13	Beulah West	550	None	Steam, 3-4	45
IBG13	Beulah West	400	None	Steam, 3-4	28
IBG13	Beluga	800	None	Steam, 3-4	88
IBG13	Beluga	800	Dolomite	Steam, 3-4	90
IBG13	Beluga	800	Zeolite	Steam, 3-4	87

TABLE 3

Uncracked Tar
(Tar_c/Tar_t)(100%)

Temp., °C	Dolomite	Zeolite
250	97	106
400	24	50
550	12	35
700	47	35*
800+	19	32

* Average of two tests.

HYDROCRACKING OF POLYOLEFINS TO LIQUID FUELS OVER STRONG SOLID ACID CATALYSTS

K. R. Venkatesh, J. Hu, J. W. Tierney and I. Wender
Department of Chemical and Petroleum Engineering
University of Pittsburgh, Pittsburgh, PA 15261

Keywords: polymer hydrocracking, solid acid, synthetic fuel

INTRODUCTION

Post-consumer plastic makes up about 13 wt% of the 48 million tons of total packaging wastes generated annually¹. Plastics are non-biodegradable, constitute a increasingly large volume of solid wastes (20 vol. % in 1990)², and are not being recycled to a significant extent³. Pyrolysis, as an alternative for plastic waste recycling, usually results in unsaturated and unstable oils of low yield and value. Significant amounts of char are formed on pyrolyzing plastic wastes.

Liquefaction of plastic wastes could be a useful way of producing desirable liquid transportation fuels. Thermoplastics such as polyethylene (PE), polypropylene (PP) and polystyrene (PS) make up the bulk of plastic wastes⁴. The liquid products obtained from them are likely to have a high volumetric energy content because of their relatively high (H/C) atomic ratio. It is known that strong liquid superacids such as Magic acid ($\text{HSO}_3\text{F}:\text{SbF}_5$) are effective in converting paraffinic wax to t-butyl cations at room temperature; however, the stability of these liquid acids is poor at the high temperatures and reducing environments⁴ needed for improving the H/C ratio of the products. In this paper, we discuss the results obtained from the hydrocracking of high density polyethylene (HDPE), PP and PS over metal-promoted sulfated zirconia catalysts, viz., $\text{Pt}/\text{ZrO}_2/\text{SO}_4$ and $\text{Ni}/\text{ZrO}_2/\text{SO}_4$. Strong solid acids such as these and other anion-modified metal oxides are active in a variety of acid-catalyzed hydrocarbon reactions^{5,6,7,8,9}; they are environmentally benign, non-corrosive (unlike strong liquid acids) and are easily separated from product streams. They are also characterized by long-term activity in the presence of hydrogen¹⁰ in reactions such as n-butane isomerization.

EXPERIMENTAL

The sulfated zirconium oxides were prepared as described in a previous publication¹¹. Incorporation of Ni on to sulfated zirconia was achieved using wet impregnation of $\text{Ni}(\text{NO}_3)_2$ followed by drying at 110°C overnight and calcination at 600°C for three hours. The amounts of Pt and Ni promoted onto ZrO_2/SO_4 were 0.5 wt% and 2.0 wt% respectively, based on the final weight of the catalyst. HDPE (density 0.95, $M_{wv} = 125,000$), PP (isotactic, density 0.85, $M_{wv} = 250,000$) and PS ($M_{wv} = 280,000$) were obtained from Aldrich Chemicals Inc. and were used as received. A $\text{Pt}/\text{Al}_2\text{O}_3$ catalyst (1 wt% Pt) was purchased from Aldrich and was activated at 450°C in air for one hour before use. All of our polymer reaction studies were conducted in a 27 cc stainless steel microautoclave attached to a 15 cc reactor stem. The catalysts were activated at 450°C in air for one hour before use; to minimize exposure to moisture, they were then charged immediately into a dried (110°C) reactor which was then quickly sealed. After cooling to room temperature, the reactants were added through the reactor stem. The feed to catalyst ratio was 5:1 by weight in all experiments. The reaction pressure (initial) at 325°C and 1200 psig (cold) H_2 were 1835 psig; initial reaction pressures at 375°C experiments for 1200 psig (cold) H_2 and 750 psig (cold) H_2 were 1930 psig and 1210 psig respectively. The reaction products were analyzed using a GC-MS (Hewlett Packard 5970B) and a gas chromatograph (Hewlett Packard 5890 II) with an FID detector.

Simulated distillations of products obtained were conducted using an HP 5890 Series II gas chromatograph (with a TCD detector) controlled by a HP 3396A integrator which is programmed to run the ASTM D2887 distillation method. The entire product mixture is dissolved in carbon disulfide (CS_2) to form a homogeneous mixture; CS_2 is not detected by the TCD detector of the simulated distillation unit. The result is given as a series of boiling points, one after every 5 wt% of the sample is eluted. Sulfur analyses of the catalyst samples were performed by Galbraith Laboratories, Inc.

RESULTS AND DISCUSSION

Hydrocracking of HDPE at 325°C (1200 psig (cold) H_2 , 60 min.) over the $\text{Pt}/\text{ZrO}_2/\text{SO}_4$

catalyst gave a 25 wt% conversion, mainly to gases (C_1 - C_6 alkanes), perhaps due to poor mass transfer during reaction so that liquid products from the initial cracking of HDPE underwent multiple cracking to gases. When HDPE was reacted at 375°C and 1200 psig (cold) H_2 (for 25 min.) over the same catalyst, more than 99 wt% of HDPE could be converted to liquids (69 wt%) and C_1 - C_6 gases (~30 wt%) (Table I). Total conversion was based on solid recovered which likely consisted of polyethylene molecules of shorter chain length than the starting HDPE. When the same reaction was conducted with a Ni/ZrO₂/SO₄ catalyst, HDPE conversion exceeded 96 wt% with slightly different liquid and gas yields (Table I). Table II lists the detailed product distribution of the liquid products formed from the reaction of HDPE over Pt/ZrO₂/SO₄ and Ni/ZrO₂/SO₄ catalysts, for the results shown in Table I. Large amounts of isoparaffins are obtained for each carbon number, close to an order of magnitude higher than their straight-chain counterparts. The high iso-/normal alkane ratios obtained at these temperatures is due to a kinetic rather than a thermodynamic effect. The more stable branched carbenium ions could abstract a hydride ion from an oligomeric fragment or react with hydride ions formed from the dissociation of molecular hydrogen over the metal as suggested by Iglesias et al.¹² and are thus easily desorbed from the catalytic sites before an equilibrium is reached.

Impregnation of Ni on ZrO₂/SO₄ resulted in a higher iso/normal ratio of C_4 - C_9 alkanes from HDPE than that obtained with Pt. This may be due to the lower hydrogenation activity of Ni (based on n-hexadecane hydrocracking experiments¹³) resulting in correspondingly lower concentration of hydride ions on the catalyst surface; the adsorbed carbocations could undergo a higher degree of skeletal transformation before desorption from the active sites by hydride transfer.

Hydrocracking of HDPE over a Pt/ZrO₂/SO₄ catalyst was conducted with a lower hydrogen pressure (750 psig (cold)) with other conditions the same as in Table I. The same total conversion (99 wt%) was obtained in this reaction but with a higher yield of liquid products (79.8 wt%) and a correspondingly lower yield of gases (19.2 wt%). Comparison of the liquid products from HDPE reactions at both values of hydrogen pressure are given below.

Reactions with PP were conducted under the comparatively milder temperature of 325°C in the presence of 1200 psig (cold) H_2 ; at these conditions, PP was converted almost entirely to C_1 - C_6 gases for a reaction time of one hour. When the reaction time was reduced to 20 minutes, PP conversion was ~100 wt% with about 90 wt% yield of liquid products. Product analysis showed (Table III) that 78.6 wt% of C_5 - C_{12} gasoline range compounds were present in the liquid products together with 11.4 wt% products in the diesel range (C_{13} - C_{20}). Similar results were obtained with a Ni/ZrO₂/SO₄ catalyst in the reaction of PP (Table III). It appears that at sufficiently high temperatures, the hydrogenation activity of Ni approaches that of Pt in these reactions. It was found earlier that, in hydrocracking of n-hexadecane at milder conditions (160°C, 350 psig (cold) H_2), Ni/ZrO₂/SO₄ showed little activity whereas high conversions were obtained with a Pt/ZrO₂/SO₄ catalyst¹⁴. A cheaper, non-noble metal such as Ni can be effective in these reactions but requires a higher temperature for activation by hydrogen. As was the case with HDPE, high ratios of iso/normal paraffins was obtained. We found that PS could also be converted to benzene, alkylated aromatics and bicyclics at 300°C with 1200 psig (cold) H_2 .

The reaction of polypropylene at 325°C and 1200 psig (cold) H_2 over a ZrO₂/SO₄ (in the absence of either Pt or Ni) catalyst which has strong acidity but no hydrogenation function, resulted in no appreciable conversion of polypropylene. The white ZrO₂/SO₄ catalyst turned black during reaction indicating deactivation, possibly by coking. This result confirms the finding by others^{5,12} that the presence of a hydrogenation metal on ZrO₂/SO₄ provides stability to the catalyst by resisting coke formation in a variety of hydrocarbon reactions. On the other hand, a one wt% Pt supported on γ -Al₂O₃ catalyst (strong hydrogenation function but weak acidic function) also gave almost no conversion of PP at 325°C and 1200 psig (cold) H_2 . It appears that at the conditions employed for hydrocracking of these polymers, both strong acid and hydrogenation functions are required for high yields of low molecular weight branched alkanes in the gasoline range.

We conducted simulated distillations of the product mixtures from polymer hydrocracking reactions to analyze their boiling point characteristics. The boiling point distribution of the liquid products obtained from the hydrocracking of HDPE (Table 3) at 375°C for 25 minutes over Pt/ZrO₂/SO₄ under two different initial hydrogen pressures are shown in Figure 1. Reactions under 750 psig (cold) H_2 and 1200 psig (cold) H_2 seem to have only a marginal effect on the boiling ranges of the liquid products obtained. More than 90 wt% of the products are in the gasoline (C_5 - C_{12}) range (i.e., between 90°F (32.2°C) and 421°F

(216.1°C)) indicating the possibility of converting HDPE to a high quality liquid fuel. A similar boiling point curve was also obtained from the simulated distillation of the products from PP over Pt/ZrO₂/SO₄; more than 70 wt% of the products obtained boil in the gasoline range. A strong tendency towards isomerization over these metal-promoted sulfated zirconia catalysts was observed for both HDPE and PP hydrocracking; this is reflected by the similar boiling point curves obtained from products of both polymers.

Despite the high activity of the sulfate-modified zirconia catalysts in these reactions, they have questionable long-term stability at these severe reducing conditions. Sulfur analyses of the catalysts after hydrocracking of HDPE revealed that the catalysts lost about 34 wt% of their starting sulfur contents during reactions at 375°C and in the presence of high H₂ pressures. Since the presence of SO₄²⁻ anions on the catalyst surface is responsible for the strong acidity of these catalysts, loss of sulfur during reaction implies loss of activity for longer periods of time.

CONCLUSIONS

Sulfate-modified metal oxides promoted by a hydrogenation metal exhibit high activities for the hydrocracking of HDPE, PP and PS. While HDPE and PP are cracked predominantly to gasoline range branched alkanes (C₅-C₁₂), PS is hydrocracked to benzene, alkylated aromatics and bicyclic compounds. Impregnation with a non-noble metal such as Ni, which showed little activity in alkane hydrocracking at milder conditions (160°C and 350 psig (cold) H₂) resulted in high activity for polymer hydrocracking at 325°C+, indicating that activation of Ni occurs at higher temperatures. The long-term stability of these catalysts for these reactions is in doubt due to their loss of sulfur. Novel catalyst formulations which have higher stability under severe reducing conditions are currently being investigated.

ACKNOWLEDGMENTS

The financial support of this work by the U.S. Department of Energy (Grant No. DE-FG22-93PC93053) is gratefully acknowledged.

REFERENCES

1. R. J. Rowatt, "The Plastics Waste Problem", Chemtech, Jan. 1993, 56-60.
2. U.S. Environmental Protection Agency (EPA) Office of Solid Waste. "Characterization of Municipal Solid Waste in the United States: 1990 Update" Publ. No. EPA/530-SW-90-042A. Washington, D.C., 1990.
3. S.G. Howell, J. Hazard. Matl., **29** (1992) 143-164.
4. G.A. Olah, G.K. Surya Prakash, and J. Sommer, Superacids, John Wiley & Sons, New York, 1985.
5. K. Tanabe and H. Hattori, Chem. Lett., (1976) 625.
6. M. Hino and K. Arata, Chem. Lett., (1981) 1671.
7. K. Arata and M. Hino, React. Kinet. Catal. Lett., (1988) 1027.
8. H. Matsuhashi, M. Hino and K. Arata, Chem. Lett., (1988) 1027.
9. K. Ebitani, H. Konno, T. Tanaka, H. Hattori, J. Catal., **135** (1992) 60-67.
10. Tanabe, K., Hattori, H. and Yamaguchi, T., Crit. Rev. Surf. Chem., **1** (1) (1990) 1-25.
11. M. Y. Wen, I. Wender and J. W. Tierney, Energy & Fuels, **4** (1990) 372-379.
12. E. Iglesia, S.L. Soled and G.M. Kramer, J. Catal., **144** (1993) 238.
13. K.R. Venkatesh, J.W. Tierney and I. Wender, unpublished results.
14. W. Wang, Ph.D. dissertation, University of Pittsburgh, 1994.

Table I Product (alkane) distributions obtained from HDPE hydrocracking over Pt/ZrO₂/SO₄ (0.5 wt% Pt) and Ni/ZrO₂/SO₄ (2.0 wt% Ni). Reaction conditions: 375°C, 1200 psig (cold) H₂, 25 min. Conversion is based on recovered solid.

PRODUCT	Yield (wt%) obtained with	
	Pt/ZrO ₂ /SO ₄	Ni/ZrO ₂ /SO ₄
Conversion	99 wt%	98 wt%
Gases (C1-C6)	30.0	28.0
Liquids:		
C4-C12	68.7	67.6
C13-C20	0.3	2.4
C21 and above	trace	trace

Table II Composition of liquid products from HDPE hydrocracking over Pt/ZrO₂/SO₄ and Ni/ZrO₂/SO₄ catalysts at 375°C, 1200 psig (cold) H₂, 25 min.

PRODUCT	YIELD (wt%) of ISO-(NORMAL) ALKANES	
	Pt/ZrO ₂ /SO ₄	Ni/ZrO ₂ /SO ₄
C4	3.6 (1.0)	2.5 (0.1)
C5	13.9 (4.8)	8.5 (0.1)
C6	25.3 (5.7)	13.5 (0.7)
c-C6	3.0	trace
C7	14.8 (2.2)	16.4 (0.8)
c-C7	3.5	1.6
C8	10.6 (0.8)	15.1 (0.5)
c-C8	0.4	0.9
C9	6.2 (0.3)	14.1 (0.4)
c-C9	trace	0.8
C10	2.4 (0.1)	10.4 (0.3)
C11	1.0 (trace)	6.3 (trace)
C12	0.3 (trace)	3.5 (trace)
C13	trace	2.2 (trace)
C14	trace	0.9 (trace)
C15-C20 (iso+normal)	trace	0.3
C21 and above (iso+normal)	trace	trace
TOTAL	85.0 (14.9)	96.2 (3.7)

Table III Results from PP hydrocracking over sulfated zirconia catalysts promoted with 0.5 wt% of Pt and with 2.0 wt% Ni. Reaction conditions were 325°C, 1200 psig (cold) H₂, 20 min. PP conversion was near 100 wt% for both reactions.

PRODUCT	Yield (wt%) obtained with	
	Pt/ZrO ₂ /SO ₄	Ni/ZrO ₂ /SO ₄
Gases (C1-C6)	10.0	14.5
Liquids:		
C4-C12	78.6	76.0
C13-C20	11.4	9.5
C21 and above	trace	trace

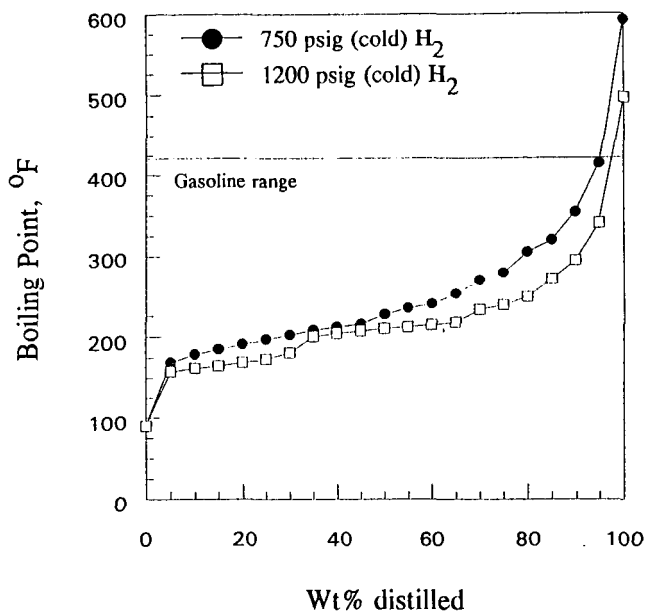


Figure 1 Boiling point curves obtained from the simulated distillation of products from HDPE hydrocracking over a Pt/ZrO₂/SO₄ catalyst at 375°C for 25 minutes under two different initial H₂ pressures.